World Academy of Science, Engineering and Technology
International Journal of Industrial and Manufacturing Engineering
Vol:9, No:1, 2015

Calculation Analysis of an Axial Compressor Supersonic Stage Impeller

Y. B. Galerkin, E. Y. Popova, K. V. Soldatova

Abstract**—**There is an evident trend to elevate pressure ratio of a single stage of a turbo compressors - axial compressors in particular. Whilst there was an opinion recently that a pressure ratio 1,9 was a reasonable limit, later appeared information on successful modeling tested of stages with pressure ratio up to 2,8. The authors recon that lack of information on high pressure stages makes actual a study of rational choice of design parameters before high supersonic flow problems solving. The computer program of an engineering type was developed. Below is presented a sample of its application to study possible parameters of the impeller of the stage with pressure ratio 3,0. Influence of two main design parameters on expected efficiency, periphery blade speed and flow structure is demonstrated. The results had lead to choose a variant for further analysis and improvement by CFD methods.

Keywords**—**Supersonic stage, impeller, efficiency, flow rate coefficient, work coefficient, loss coefficient, oblique shock, direct shock.

NOMENCLATURE

B	chord length
B_f	distance along chord to the point of maximum camber
$h_T = c_{u2} \cdot u$	head (no swirl at an inlet)
k	isoentropic coefficient
l	blade length
M	Mach number
p	pressure
$\tilde{p}^*$	total pressure in rotating coordinates
r	radius
R	gas constant
t	blade pitch
T	temperature
T^*	total temperature
u	blade speed
β_{bl}	blade angle related to tangential direction
β	flow angle related to tangential direction
$\varepsilon = \beta_2 - \beta_1$	flow deflection angle
φ	flow rate coefficient
γ	oblique shock angle
$\eta^* = \dfrac{\ln \pi^*}{\dfrac{k}{k-1}\ln\left(\dfrac{T_2^*}{T_1^*}\right)}$	impeller total efficiency
λ	velocity coefficient
π^*	total pressure ratio
ρ	gas density
$\theta = \beta_{bl2} - \beta_{bl1}$	camber angle
ψ_T	work coefficient
$\varsigma = \dfrac{h_{w\,subsonic}}{0,5w_{1\,subsonic}^2}$	loss coefficient of an impeller subsonic part
$\Delta\beta = \beta_{bl2} - \beta_2$	deviation angle

Subscripts

1	impeller inlet
2	impeller exit
h	rotor surface (blade root)
s	body surface (blade periphery),
sonic	parameters after shocks

Yuri Borisovich Galerkin is with S.-Peterbugd Poltechnical Yniversity, Russian Federaton (phone: +7-921-942-73-40; fax: 8-812-552-86-43; e-mail: yuiri_galerkin@mal.ru).
Elena Yrievna Popova is with S.-Peterbugd Poltechnical Yniversity, Russian Federaton (phone: +7-931-224-93-94 fax: 8-812-552-86-43; e-mail: buck01@list.ru).
Kristna Valerievna Soldatova is with S.-Peterbugd Poltechnical Yniversity, Russian Federaton (phone: +7-905-220-50-70, fax: 8-812-552-86-43; e-mail: buck02@list.ru).

I. OBJECTS AND MAIN EQUATIONS

Fig. 1 shows an impeller scheme with 20 blade-to-blades surfaces to calculate flow vectors and parameters along blade length.

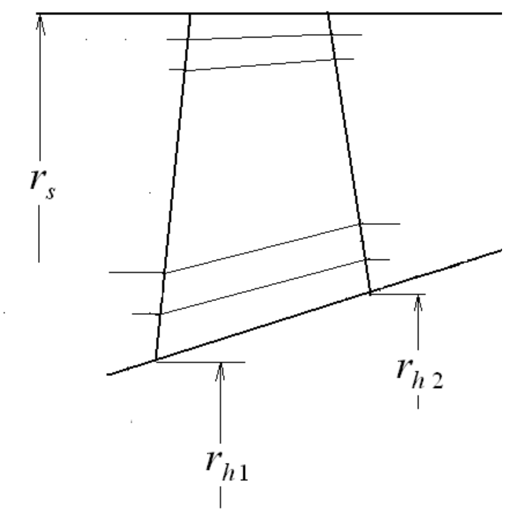

Fig. 1 Scheme of an impeller with blade to blade surfaces for flow parameter calculation

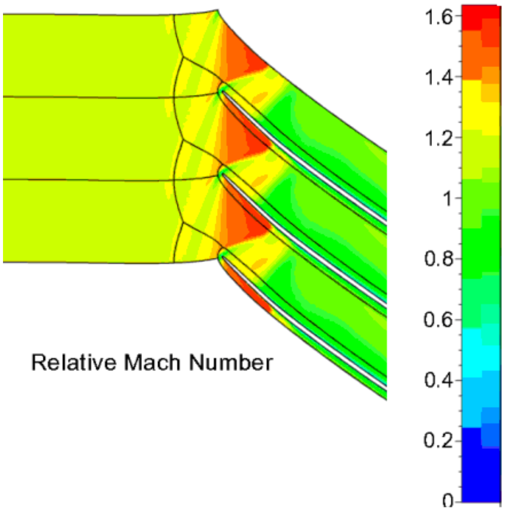

Fig. 2 Relative Mach number at an inlet of a compressor cascade

These are main equations for impeller parameters analysis. Blade periphery speed that is necessary to obtain given pressure ratio is connected with the velocity coefficient, work coefficient and efficiency:

$$\lambda_u = \frac{u_s}{\sqrt{\frac{2kRT_1^*}{k+1}}} = \left(\frac{\pi^{*\frac{k-1}{k\eta^*}} - 1}{2\frac{k-1}{k+1}\psi_{Ts}} \right)^{0.5}. \tag{1}$$

Here efficiency and pressure ratio are calculated at each blade to blade surface and are averaged. Calculations are made with conditions $c_z(r) = const$, $c_{u1} = 0$.

The condition $c_u \times r = const$ along radii guarantees flow radial equilibrium for an ideal homogenous stage and is widely applied to real subsonic impellers [1]. It cannot be applied to a supersonic impeller due to sufficient difference of shock losses along radii. Iterative process is applied to fulfill the radial equilibrium condition:

$$\frac{\partial p}{\partial r} = \rho \frac{c_u^2}{r}. \tag{2}$$

Calculation starts with some estimated value of $\psi_{Ts} = c_{u2s}/u_s$. Static pressure at an outer radius p_{2s} is calculated meaning its rise in supersonic shocks and polytypic compression in a subsonic part of a blade channels. Static pressure at a below blade to blade surface is calculated by (2). Corresponding value of c_{u2} at this surface is evaluated iteratively. Averaged pressure ratio π^* is calculated and is compared with given data. Iterations follow to obtain given pressure ratio.

Classic gas dynamic formulae are applied to calculate flow parameters after supersonic shocks at each blade-to-blade surfaces. An oblique shock angle γ depends on Mach number and leading edge sharpness. Minimum angle γ_0 corresponds to a sound wave:

$$sin\gamma_0 = \frac{1}{M_1}. \tag{3}$$

Authors' CFD calculations have shown that while a velocity coefficient is high enough an oblique shock is followed with a direct one. Fig. 2 represents a typical structure.

The calculations below are made at supposition that angle γ has a mean value between γ_0 and 90^0. The loss of total pressure in an oblique shock depends on a velocity coefficient normal to an oblique shock front:

$$\frac{\tilde{p}_s^*}{\tilde{p}_1^*} = \frac{1}{1+\left(\lambda_{1n}^2 - 1\right)}\lambda_{1n}^2 \left[\frac{1-\frac{k-1}{k+1}\lambda_{1n}^2}{1-\frac{k-1}{k+1}\cdot\frac{1}{\lambda_{1n}^2}} \right]^{\frac{1}{k-1}}. \tag{4}$$

Velocity coefficients after oblique and direct shocks:

$$\lambda_s = \sqrt{\lambda_1^2\cos^2\gamma + \frac{\left(1-\frac{k-1}{k+1}\lambda_1^2\cos^2\gamma\right)^2}{\lambda_1^2\left(1-\cos^2\gamma\right)}}, \tag{5}$$

$$\lambda_{sonic} = \frac{1}{\lambda_s}. \tag{6}$$

The authors of [2]-[4] analyzed different empirical formulae developed on the base of subsonic blade cascade wind tunnel tests. The conclusion was that calculation method proposed at [5] is most completed and estimates efficiency of multistage subsonic compressors rather well. The equations of [5] are applied to calculate subsonic part of a stage.

Coefficient of profile losses depends on a camber angle, a flow inlet angle and a relative spacing:

$$\zeta_p = \frac{0,65 + 2\left(\frac{\theta}{100}\right)^2}{100\sqrt{\sin\beta_1}\cdot(t/B)}. \tag{7}$$

A camber angle depends on a flow deflection $\varepsilon = \beta_2 - \beta_1$ necessary to obtain given pressure ratio, a deviation angle and an incidence angle at a design flow rate:

$$\theta = \varepsilon + \Delta\beta - i. \tag{8}$$

A deviation angle on profiles:

$$\Delta\beta_p = \left[0,26\left(2\frac{B_f}{B}\right)^2\left(\frac{t}{B}\right) + 0,2\frac{\beta_2}{100}\right]\theta \cdot \quad (9)$$

An additional deviation angle due to flow along hub and shroud surfaces

$$\Delta\beta_h = 2,5\left(ctg\beta_1 - ctg\beta_2\right)\frac{(t/B)}{(l/B)}\sin\beta_2 \cdot \quad (10)$$

The full deflection angle is

$$\Delta\beta = \Delta\beta_p + \Delta\beta_h .$$

Incidence angle at a design flow rate:

$$i_1 = 6 - \frac{1}{3}\theta(t/B)\left[1,81 - \left(2\frac{B_f}{B}\right)^2\right] - 6\left[1 - \left(1 - \frac{\theta}{60}\right)^2\right]. \quad (11)$$

Loss coefficient at hub and shroud surfaces:

$$\zeta_0 = \zeta_p \frac{(t/B)}{(l/B)} \cdot \quad (12)$$

Loss coefficient due to secondary flow at hub and shroud surfaces:

$$\zeta_i = 0,10\left(ctg\beta_1 - ctg\beta_2\right)^2 \sin\beta_1 \frac{(t/B)}{(l/B)} \cdot \quad (13)$$

An impeller subsonic part loss coefficient is a sum:

$$\zeta = \zeta_p + \zeta_0 + \zeta_i \quad (14)$$

The equations above demonstrate importance of exit and inlet flow angles. On periphery of blades inlet angle is equal if c_{u1}=0:

$$\beta_{1s} = arctg\varphi_{1s} \cdot \quad (15)$$

Work coefficient depends on flow rate coefficient, axial velocity deceleration in an impeller and flow exit angle:

$$\psi_{Ts} = 1 - \varphi_{1s}\frac{c_{z2}}{c_{z1}} ctg\beta_{2s}, \quad (16)$$

where $\beta_{2s} = \beta_{1s} + \varepsilon_s$.

II. Data on Existing High Pressure Stages

The typical values of modern high pressure supersonic stages work coefficient are presented in Table I - the reduced data. Assumed values at calculations were: η^*_{ad} = 0,87, k=1,4, R= 287,3 J/kg /K, T^*_0 = 288 K.

There is an evident rend to achieve higher pressure ratio by elevation of the work coefficient but not by blade periphery speed. Let us note that the stage with π^*= 1,82 has ψ_{Ts}= 0,300 - the value typical for subsonic stages. The stage with π^*= 2,80 has much higher ψ_{Ts}= 0,562 – as many of industrial centrifugal impellers. Its periphery blade speed is slightly less than in case of the stage with π^*= 1,82.

TABLE I
Work Coefficient Estimation of Modern High Pressure Axial Stages

π^*	u_s (m/s)	$h_T = \frac{kRT_1^*((\pi^*)^{\frac{k-1}{k}} - 1)}{(k-1)\eta^*_{ad}}$	$\psi_{Ts} = \frac{h_T}{u_s^2}$
1,6	370	47810	0,349
1,82	455	62080	0,300
1,9	370	66960	0,489
2,05	455	75850	0,366
2,25	420	86740	0,492
2,55	440	102000	0,527
2,8	450	113780	0,562

The evident advantages of lower periphery speed are lower mechanical stresses in rotor details. The influence of high work coefficients on efficiency is not so evident. The Authors preliminary calculations have demonstrated that elevation of work coefficient (15) by the ratio c_{z2}/c_{z1} diminishing is not rational. The elevation of flow deflection angle $\varepsilon = \beta_2 - \beta_1$ is necessary. It is not recommended for subsonic stages though.

III. Stage Parameters Analysis

The influence of two important design parameters ε_s and φ_{1s} on the impeller of the stage with pressure ratio π^*= 3,0 demonstrate graphics below. Constant design parameters are: c_{z2} / c_{z1} = 0,80, l/B = 1,20, D_h/D_s = 0,60.

There is a popular opinion that supersonic stages can operate successfully with minimal deflection angles as flow deceleration c_{z2}/c_{z1} provides necessary work coefficient. It is not so when the necessary pressure ratio is as high as 3,0. Fig. 3 shows that at ε_s < 8^0 periphery blade speed level u_s is unacceptable.

The less is flow coefficient at given ε_s the lower is periphery blade speed. Shown at Fig. 3 work coefficient values at ε_s = 12^0 are close to high pressure stages in the Table I.

The reason of efficiency decline at higher velocity coefficients are losses in shocks. Total efficiency and inlet Mach numbers are presented at Fig. 4. Let us notice that at

$\varepsilon_s = 8^0$ impeller total efficiency is equal at φ_s =0,30 and 0,35. Flow inlet angle β_{1s} = 16,7^0 corresponds to flow rate coefficient φ_{1s} =0,30. Blade inlet angle is still lesser as the incidence angle is negative. Test CFD calculation of authors has shown that flow character was dubious at the small value of β_{bl1s}. The variant with φ_s = 0, 35 seems to be more attractive as the inlet flow angle is bigger. Value of η^*=0,92 is quite satisfactory for the impellers of the stage with π^* = 3,0.

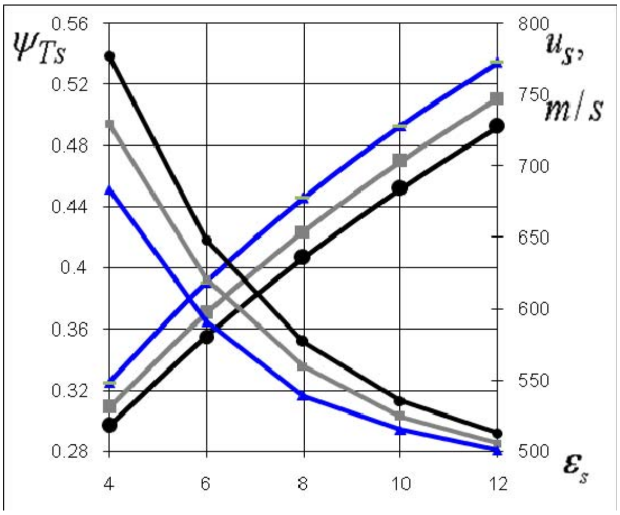

Fig. 3 Periphery blade speed and work coefficient versus periphery deflection angle and flow rate coefficient

● - φ_s =0,4, ■ - φ_s =0,35, ▲ - φ_s =0,3.

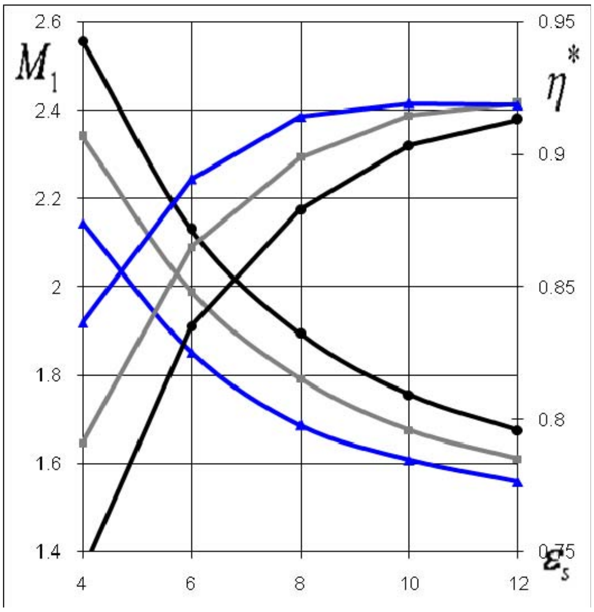

Fig. 4 Impeller total efficiency versus periphery deflection angle and flow rate coefficient ● - φ_s =0,4, ■ - φ_s =0,35, ▲ - φ_s =0,3.

The bigger are flow rate and blade speed the higher are inlet Mach numbers. To the contrary, the efficiency is higher while lower are flow rate and blade speed – Fig. 4.

As it will be shown later the smaller are ε_s the lower are loss coefficients at the subsonic part of the impeller. Evidently shock losses prevail in impellers of a stage with the pressure ratio 3,0.

IV. Flow Parameters along Blade Height

Some information on flow parameters along blade height for variants with φ_s = 0, 35 and different ε_s are presented below.

Inlet Mach numbers along relative radius are presented at Fig. 5.

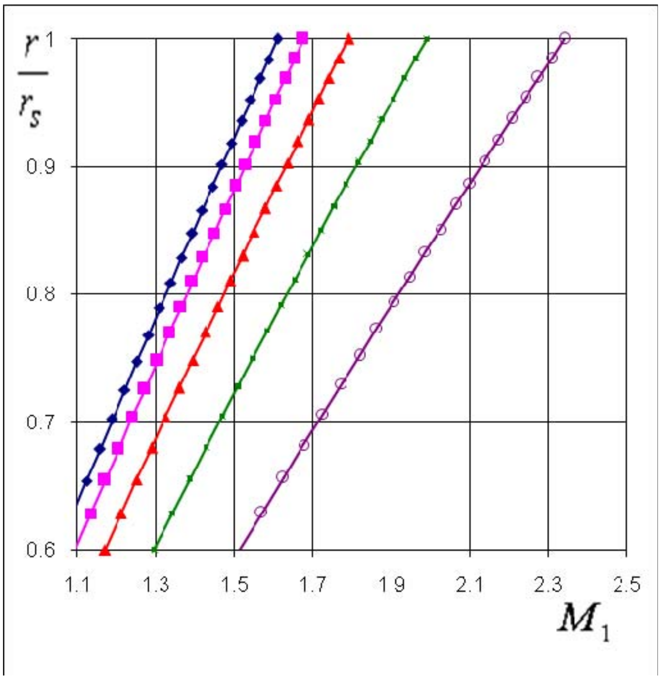

Fig. 5 Inlet Mach number along relative radius φ_s =0,35. Flow deflection angles 4, 6, 8, 10, 120 from right to left

Periphery Mach number exceeds 2,3 in case of $\varepsilon_s = 4^0$. Evidently, small deflection angles are not acceptable because of it.

Total pressure drop in oblique/direct shocks along relative radius is presented at Fig. 6. Pressure loss is 10 – 36% for r/r_s = 0,6 – 1,0 in case of $\varepsilon_s = 4^0$ that is too much.

Loss coefficient of the impeller subsonic part along relative radius for deflection angles 4, 6, 8, 10, 12^0 is presented at Fig. 7.

Small flow deflection and low Mach number at the inlet to subsonic part lead tp small loss coefficients when $\varepsilon_s < 10^0$.

Too high losses in shocks in these cases lead to lower efficiency of the impeller as is shown at Fig. 8.

Exit flow angle along relative radius are presented at Fig. 8.

For subsonic impellers flow exit angles $\beta_2 < 60^0$ are recommended but there is no limitation foe supersonic ones. Value $\beta_2 = 90^0$ for $\varepsilon_s = 12^0$ is not excessive.

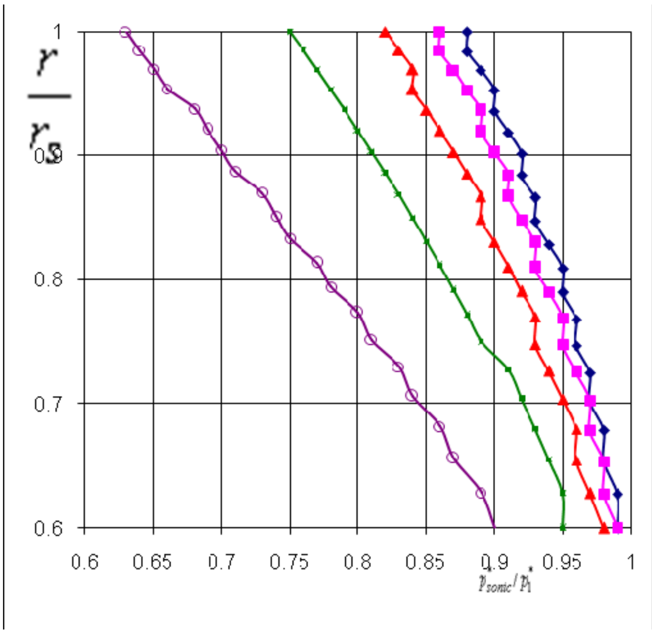

Fig. 6 Total pressure drop in oblique/direct shocks along relative radius φ_s=0,35. Flow deflection angles 4, 6, 8, 10, 120 from left to right

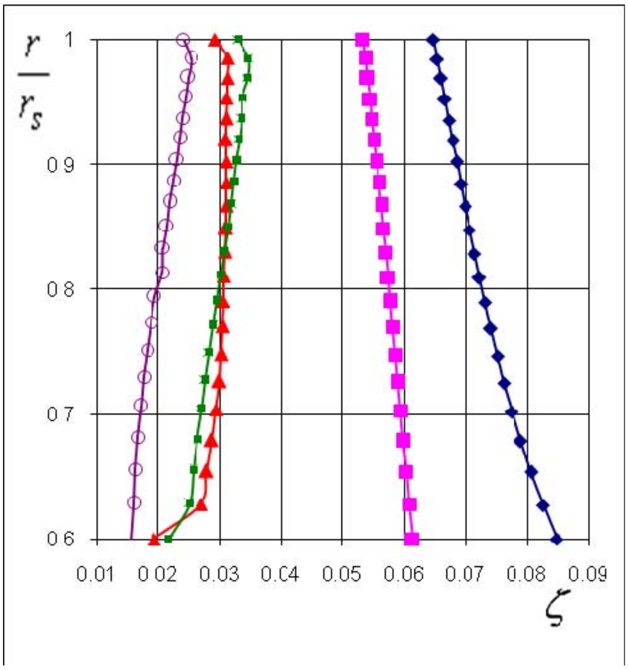

Fig. 7 Loss coefficient of the impeller subsonic part along relative radius φ_s=0,35. Flow deflection angles 4, 6, 8, 10, 12^0 from left to right

There is understanding that many problems are out of the analytical abilities of the described method. Authors' opinion is that its validity is limited by general analysis of impeller candidates. The information for blade design is presented by the computer program as β_{bl12}, $\beta_{bl2} = f(r)$. CFD calculations and corrections are the next steps of gas dynamic design.

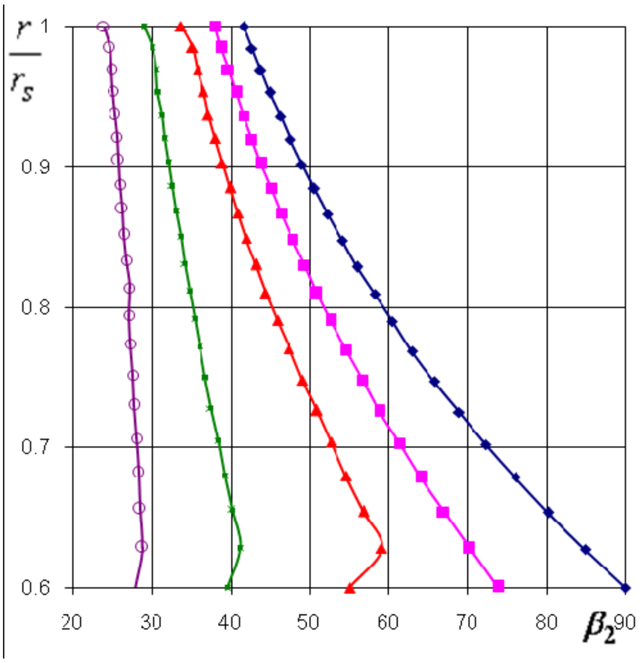

Fig. 8 Exit flow angle along relative radius φ_s=0,35. Flow deflection angles 4, 6, 8, 10, 120 from left to right

References

[1] Galerkin, Y.B Turbocompressors. - Moscow. - 2010. – C. 596. (in Russian)

[2] Galerkin Y. B., Popov Y. A. Optimization of the axial compressors flow path at a stage of candidates' comparison. Part 1. // Compressors & Pneumatics. – Moscow. - 2009. – No.5. – P.2-9 (in Russian).

[3] Galerkin Y. B., Popov Y. A. Optimization of the axial compressors flow path at a stage of candidates' comparison. Part 2. // Compressors & Pneumatics. – Moscow. - 2009. – No.6. – P.1-19 (in Russian).

[4] Galerkin Y. B., Popov Y. A. Optimization of the axial compressors flow path at a stage of candidates' comparison. Part 3. // Compressors & Pneumatics. – Moscow. - 2009. – No.7. – P. 6-12 (in Russian).

[5] Komarov A.P. Axial blade cascades test. Turbo machines and jet apparatus. – Moscow. –1967. – C. 67-110. (in Russian).